Binding-Dependent Disorder−Order Transition in PKIα: A Fluorescence Anisotropy Study†

Jennifer A. Hauer,‡ Susan S. Taylor,‡ and David A. Johnson,*,§

Department of Chemistry and Biochemistry and the Howard Hughes Medical Institute, University of California, San Diego, La Jolla, CA, 92093-0654, and Division of Biomedical Sciences, University of California, Riverside, Riverside, CA, 92521-0121

Received December 30, 1998; Revised Manuscript Received April 12, 1999

ABSTRACT: The conformational flexibility of peptidyl ligands may be an essential element of many peptide−macromolecular interactions. Consequently, the α-carbonyl backbone flexibility of the 8 kDa protein kinase inhibitor (PKIα) peptide of cAMP-dependent protein kinase (cAPK) free in solution and bound to cAPK was assessed by time-resolved fluorescence anisotropy. Specifically, three full-length, single-site PKIα mutants (V3C, S28C, and S59C) were prepared, and fluorescein iodoacetamide (FI) was selectively conjugated to the side chains of each substituted cysteine. The time-resolved anisotropy decay profiles of the labeled mutants were well fit to a model-free nonassociative biexponential equation. Free in solution, the three labeled proteins had very similar anisotropy decays arising primarily from local α-carbonyl backbone movements. Only a small fraction of the anisotropy decay was associated with slower, whole-body tumbling, confirming that PKIα is highly disordered at all three locations. Complexation of the mutants with the catalytic (C) subunit of cAPK decreased the rate of whole-body tumbling for all three mutants. The effects on the rapid decay processes, however, were dependent upon the site of conjugation. The anisotropy decay profiles of both FI-V3C- and FI-S28C-PKIα were associated with significantly reduced contributions from the fast decay processes, while that of FI-S59C-PKIα was largely unaffected by binding to the C-subunit. The results suggest that the cAPK-binding domain of PKIα extends from the its N-terminus to residues beyond Ser^{28} but does not include the segment around Ser^{59}, which is still part of a highly flexible domain when bound to the C-subunit.

Ligand flexibility plays a crucial role in many high-affinity bimolecular interactions. Conformational disorder within free ligands in solution can affect binding interactions in at least three ways. First, ligand flexibility can increase the binding affinity through a net entropy gain from the binding-associated reduction in surface area of the disordered ligand and the subsequent mobilization of the ordered water molecules located around the ligand (*1*). Second, conformational flexibility can enhance the association rate by permitting more rapid sampling of ligand conformations during the random ligand-target dance that precedes binding. Finally, conformational flexibility can broaden substrate specificity by increasing the number of functional ligand conformations (*2*, *3*).

An example of a conformationally flexible ligand is the protein kinase inhibitor, PKIα. Within its 75 amino acid sequence are two functional domains: a competitive inhibitory domain that binds to the catalytic (C)[1] subunit of cAMP-dependent protein kinase (cAPK) and a Nuclear Export Signal (NES) (Figure 1)(*4*, *5*). Residues 18−24 contain the inhibitory pseudosubstrate sequence and are preceded by residues 5−13 that enhance the binding affinity by 100-fold (*6*). The NES is sequentially separate and fully contained within residues 37−46 of PKIα (*7*).

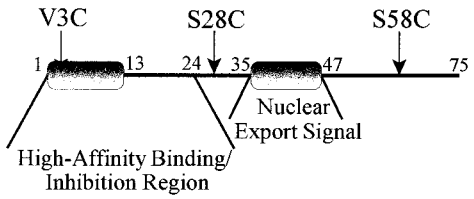

FIGURE 1: Schematic delineating the sites of fluorescein iodoacetamide labeling and their proximity to the two functional and α-helical domains (lobated cylinders) of PKIα.

The free-solution structure of full-length PKIα and two fragments, PKIα(1−25) and PKIα(26−75), have been

† This work was supported by a grant from the University of California Universitywide AIDS Research Programs (R96−SD-107) to S.S.T.

* All correspondence should be addressed to David A. Johnson, Division of Biomedical Sciences, University of California, Riverside, CA 92521-0121 (e-mail: david.johnson@ucr.edu).

‡ University of California, San Diego.

§ University of California, Riverside.

[1] Abbreviations: PKIα, the α isoform of the heat stable inhibitor of cAMP-dependent protein kinase; cAPK, cAMP-dependent protein kinase; C-subunit, the α isoform of the catalytic subunit of cAPK; FI, fluorescein iodoacetamide; FM, fluorescein maleimide; NES, nuclear export signal; TRFA, time-resolved fluorescence anisotropy; buffer A, 20 mM MOPS, 150 mM KCl, pH 7.0; buffer B, 20 mM MOPS, 150 mM KCl, 2 mM β-mercaptoethanol, 1 mM ATP, 5 mM $MgCl_2$, pH 7.0; DTT, dithiothreitol; r_o, anisotropy at time zero; r_{VF}, amplitude of "very fast" anisotropy decay process; r_F, amplitude of "fast" anisotropy decay process; r_S, amplitude of "slow" anisotropy decay process; ϕ_F, fast rotational correlation time; ϕ_S, slow rotational correlation time; τ, fluorescence lifetime.

10.1021/bi983074k CCC: $18.00
Published on Web 05/06/1999

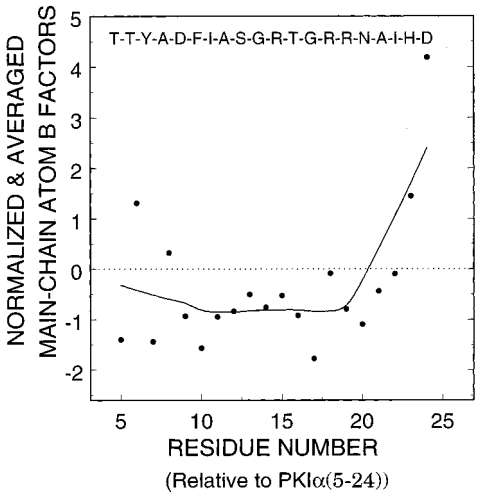

FIGURE 2: Normalized and averaged main-chain atom *B* factors of C-subunit-bound PKIα(5−24). The averaged main-chain atom *B* factors of each residue of C-subunit-bound PKIα(5−24) are presented in units of standard deviation. The raw *B* factors were taken from the Protein Data Bank (PDB) entry filename 1ATP, which contains the X-ray coordinates of murine recombinant cAPK complexed to MgATP and PKIα(5−24). The normalized *B* factors were calculated by first subtracting the average of all the main-chain atom *B* factors in the 1ATP file from the average of each PKIα(5−24) residue and then dividing the substrahend by the standard deviation of all the main-chain atom *B* factors in the 1ATP file.

examined by NMR spectroscopy (*8*). Within PKIα(1−25), the NOE data reveal a single ordered, amphipathic α-helix that extends from Thr^{1} to Ser^{13}. The remainder of PKIα-(1−25), including the pseudosubstrate site, is unstructured. For PKIα(26−75), the only identified structure is an α-helix followed by a loose turn (encompassing residues 35−47) that overlaps with the NES. Analysis of the chemical shift data of the full-length molecule confirms the presence only of these two short-structured segments (*8*).

Little is known about the conformational flexibility of PKIα in the cAPK-bound state. Some insight can be gained from an analysis of the averaged main-chain atom *B* factors found in the protein database (PDB) file of PKIα(5−24) cocrystallized with the C-subunit (*9*) (Figure 2). From such an analysis, the middle portion of this fragment (residues 9−20) is associated with main-chain atom *B* factors that are about a standard deviation below the cocrystallized C-subunit average, indicating a high level of immobility for this segment. With the exception of the last two residues (His^{23} and Asp^{24}) that have high *B* factors and are probably highly mobile, the other residues (5−8 and 20−22) are associated with *B* factors which are about average for the C-subunit, indicating somewhat more mobility than the middle portion of PKIα (5−24).

Because PKIα is believed to play a role in a growing number of cellular processes (*10*−*12*) and because conformational flexibility may be an essential element in its function, we attempted to examine in more detail the bound conformational flexibility of PKIα using fluorescence spectroscopy. Specifically, three X-to-Cys point mutants of PKIα (V3C, S28C, and S59C) were engineered and labeled at the sites of mutation with fluorescein iodoacetamide, and the time-resolved fluorescence anisotropy (TRFA) of the conjugated fluorescein was measured. The anisotropy decays were well fit to a biexponential equation. The amplitudes and rotational correlation times of the fast decay processes, which have recently been shown to correlate with the α-carbonyl backbone flexibility around each site of cysteine substitution and labeling (*13*), confirmed that PKIα is poorly structured free in solution and that the three segments of PKIα examined display differential flexibility upon binding to the C-subunit.

EXPERIMENTAL PROCEDURES

Preparation and Purification of Catalytic Subunit and Mutant PKIα's. Three X-to-Cys single-point mutations (V3C, S28C, and S59C) were introduced into wild-type PKIα by the method of Kunkel (*14*) and verified by sequencing. All three PKIα mutants were overexpressed in *Escherichia coli* and purified as described previously (*15*). The expression of the expected protein was verified by mass spectrometry, and each purified protein was lyophilized for long term storage. Recombinant C-subunit was similarly overexpressed in *E. coli* and purified as described previously (*16*). The C-subunit isoform II with three phosphorylated side chains (Ser^{10}, Thr^{197}, and Ser^{338}) was used in all experiments described below.

Fluorescein Iodoacetamide Labeling. For each mutant, lyophilized peptide was weighed out and dissolved in buffer A (degassed 20 mM MOPS, 150 mM KCl, pH 7.0) to a final concentration of 0.13 mM. Dithiothreitol (DTT) (5 mM) was added to this solution to reduce interprotein disulfide bond formation. One hour later, the dissolved protein was eluted through a NAP-10 column equilibrated with buffer A at room temperature to remove the DTT, and then quickly mixed with a 20-fold molar excess of fluorescein iodoacetamide. The reaction was allowed to proceed for 1 h at room temperature protected from light. The reaction mixture was then eluted sequentially through two NAP-10 columns (Pharmacia Biotech, Uppsala, Sweden) equilibrated with Buffer A to remove unconjugated dye. An aliquot of each sample was subjected to SDS−polyacrylamide gel electrophoresis (15%), and the fluorescent bands were visualized with a mineral lamp to verify the absence of unconjugated dye. The stoichiometric labeling of each mutant PKIα was verified by mass spectrometry.

Verification of Inhibitory Activity. The inhibitory activity of all of the PKIα conjugates was assessed by examining their ability to inhibit the phosphoryltransferase activity of cAPK using the method of Cook et al. (*17*) with 20 nM C-subunit and kemptide (100 μM) as the substrate (*17*).

Complex Preparation. Each FI-labeled PKIα mutant was preincubated with C-subunit (1:6 molar ratio) in buffer B (20 mM MOPS, 150 mM KCl, 2 mM β-mercaptoethanol, 1 mM ATP, 5 mM $MgCl_2$, pH 7.0) for 30 min prior to elution through a Superdex 75 HR 10/30 FPLC column to separate free and cAPK-bound PKIα. The column, with a one milliliter sample loop, was operated at room temperature with Buffer B as the mobile phase (flow rate = 0.8 mL/min). The UV absorbance and fluorescein emission of the eluant were monitored by a Pharmacia spectrometer (with a 280 nm interference filter) and by a Hitachi spectrofluorometer (excitation at 492 nm and emission at 515 nm), respectively.

Steady-State Emission Spectra. Steady-state emission spectra were measured with an I. S. A., Jobin Yvon-Spex FluoroMax II spectrofluorometer (Edison, NJ) with excitation

and emission slits set at 5 nm and the excitation wavelength set at 460 nm.

Time-Resolved Fluorescence Anisotropy. The time-resolved emission anisotropy was determined by the time-correlated single photon-counting technique (*18*) with an EEY scientific nanosecond spectrofluorometer (La Jolla, CA) equipped with an IBH (Edinburgh, U.K.) hydrogen-arch flash lamp. Both horizontally ($I_\perp(t)$) and vertically ($I_{||}(t)$) polarized emission decays were collected by exciting samples with vertically polarized light while orienting the emission polarizer (Polaroid HNP'B dichroic film) in either the orthogonal or vertical direction. Excitation and emission bands were selected with Oriel 500 nm short pass interference (catalog no. 59876) and Corning 3-69 cuton filters, respectively. Typically, 1×10^4 peak counts were collected (in 5−10 min) for each decay. The total counts in the orthogonal and vertical curves were scaled with respect to each other by using the steady-state ratio of integrated photon counts/6 $\times 10^6$ lamp flashes detected when the samples were excited with vertically polarized light while the emission polarizer was oriented in both directions. To minimize convolution artifacts, we recorded lamp flash profiles by removing the emission cuton filter and monitoring light scatter from a suspension of latex beads, and a depolarizing filter (DPU-25; Optics for Research, Caldwell, NJ) was placed in the emission pathway just in front of the photomultiplier. The wavelength-dependent temporal dispersion of the photoelectrons by the photomultiplier (Phillips XP2020Q) was corrected by the data analysis software. Although the polarization bias (G) of the detection instrumentation was small (1.028), it was determined by measuring the integrated photon counts/6 $\times 10^6$ lamp flashes detected, while the samples were excited with orthogonally polarized light and the emission was monitored with a polarizer oriented vertically and horizontally.

The TRFA, *r(t)*, is defined as

$$r(t) = \frac{[I_{||}(t) - GI_\perp(t)]}{[I_{||}(t) + 2GI_\perp(t)]} \quad (1)$$

Fluorescence lifetimes and correlation times were obtained through simultaneous fitting of the horizontal and vertical decay curves of each sample using the Globals Unlimited software package (Laboratory for Fluorescence Dynamics, Urbana IL) (*19*). The goodness of fit was evaluated from the values of χ^2 and visual inspection of the difference between the experimental data and an empirical nonassociative model. This model can be expressed as the sum of two exponentials,

$$r(t) = r_F \exp(-t/\phi_F) + r_s \exp(-t/\phi_s) \quad (2)$$

where r is the amplitude of the exponential decay and ϕ is the correlation time of the anisotropy decay. Subscripts F and S denote the fast and slow processes, respectively. The deconvolution analysis used data points of the emission decay profiles whose values were at least 1% of the maximum peak emission.

RESULTS

Labeling and Characterization of PKIα Mutants. The three X-to-Cys PKIα mutants (Figure 1) were overexpressed, purified to greater than 95% as assessed by visual inspection of Coomassie-stained SDS−PAGE gels and of FPLC chromatography profiles. The composition was verified by amino acid sequencing, and mass spectroscopy of each mutant PKIα was consistent with the expected fragmentation masses of the desired mutants (data not shown). The unitary stoichiometry of fluorescein iodoacetamide labeling was also verified by mass spectroscopy. SDS−PAGE analysis of the fluorescein conjugates showed no detectable nonconjugated probe. All labeled PKIα's displayed K_I's for the catalytiC-subunit <20 nM, indicating that all the conjugates bind to cAPK with substantial affinity (data not shown).

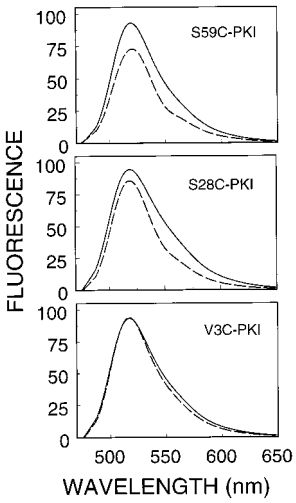

FIGURE 3: Emission spectrum of the three labeled PKIα free in solution (solid line) and complexed to the C-subunit (dashed line). Excitation was at 460 nm. Fl-V3C, Fl-S28C, and Fl-S59C are shown in the lower, middle, and upper panels, respectively.

Isolation and Characterization of FI-PKIα−C-Subunit complexes. The FI-PKIα−C-subunit complexes were well-resolved by gel filtration from the free PKIα and somewhat less well resolved from free C-subunit (data not shown). Although both the free C-subunit and FI-S28C−C-subunit complex were only partially resolved from one another, it was possible to pool the leading edge fractions of the complex so that little or no detectable amounts of the free C-subunit were present in the pooled fractions. The purity and the stability of the pooled complexes are demonstrated by the fact that re-elution of aliquots of the pooled complexes 5−7 days after their initial elution through the Superdex 75 yielded a single detectable peak of fluorescein emission and UV absorbance with unchanged retention time (data not shown).

Emission spectroscopy of the free FI-labeled mutants and FI-PKIα−C-subunit complexes indicated that binding had little effect on the emission maximum of the fluorescein conjugates. The emission maxima of the free and bound FI-labeled PKIα ranged between 516 and 518 nm whether the conjugate was bound (Figure 3). Although there were no significant chromic shifts associated with binding to the C-subunit, the quantum yields of the FI-labeled PKIα's were differentially affected by binding. The steady-state emission (Figure 3) and fluorescence lifetime (Table 1) of Fl-V3C were unchanged, while the steady-state emission (Figure 3) decreased upon binding to cAPK for both Fl-S28C and Fl-S59C 7% and 22%, respectively. Also, although the fluorescence lifetime of FI-S59C was unaffected by binding, the lifetime of FI-S28C increased from 4 to 4.4 ns upon binding

Table 1. Summary of the Best-Fit TRFA Decay Parameters for the Labeled PKIα Mutants Free in Solution and Bound to the C-Subunit[a]

	r_{VF}[b]	r_F[c]	ϕ_F[d] (ns)	r_S[e]	ϕ_S[f] (ns)	τ[g] (ns)
V3C	0.11	0.22	1.4	0.02	16	3.9
V3C−C complex	0.11	0.15	1.6	0.09	32	4.0
S28C	0.12	0.22	1.0	0.01	17	4.0
S28C−C complex	0.07	0.07	1.7	0.21	40	4.4
S59C	0.13	0.18	0.8	0.04	13	3.9
S59C−C complex	0.13	0.18	1.1	0.04	32	3.9

[a] Anisotropy decay data were fit to eq 2 with the Globals Unlimited program as described under Experimental Procedures. The average χ^2 for fitting the data to eq 2 ranged from 1.3 to 2.6. [b] The amplitude of the very fast decay process, which equals 0.35 minus r_o. The value of 0.35 was the experimentally determined r_o of fluorescein in the absence of rotational diffusion. [c] The amplitude of the fast decay process. [d] Fast rotational correlation time. [e] The amplitude of the slow decay process. [f] Slow rotational correlation time. [g] Fluorescence lifetime. The average sd's of the r terms, ϕ_F, and τ are ±0.01, ±0.2, and ±0.1 ns, respectively.

(Table 1). This binding-dependent increase in the emission lifetime of the FI-S28C mutant suggests that the fluorescein moved into a more hydrophobic environment upon binding to the C-subunit, possibly from being sandwiched between the PKIα and the C-subunit.

Time-Resolved Anisotropy Decay. TRFA directly monitors the reorientation of the emission transition dipole moment of a fluorophore in the picosecond/nanosecond time domain. When the fluorophore is conjugated to a specific protein side chain, the anisotropy decay can usually be well fit to a biexponential equation. For example, each of the anisotropy decay profiles of fluorescein maleimide (FM) conjugated to five exposed and substituted cysteines in the 40 kDa C-subunit of cAPK is associated with "slow" and "fast" decay processes. In addition to these decay processes, there are "very fast" decay processes that represent subnanosecond angular excursions of the fluorophore the rates of which are above the quantification limits of most instruments.

In the case of the FM-labeled C-subunits of cAPK, the rate of the slow decay processes is attributable to the whole-body rotational correlation time. The rate and the amplitude of the fast decay processes are respectively negatively ($r \approx -0.88$) and positively ($r \approx 0.40$) correlated with the averaged main-chain atom crystallographic temperature (or *B*) factors around each site of conjugation (see Figure 4 in ref *13*). Because *B* factors are proportional to the mean-square displacement of the atoms from their rest positions and vary with vibrational displacement, crystal disorder, and errors in the structural model, the rate and to a lesser extent the amplitude of the fast anisotropy decay processes associated with FM conjugates largely monitor α-carbonyl backbone flexibility of solvent-exposed sites on cAPK and possibly other similarly labeled proteins.

The time-resolved emission and anisotropy decay profiles of the three FI-labeled PKIα mutants both free in solution and complexed to the C-subunit are illustrated in Figures 4−6. All of the emission decays (upper panels) were well fit to a monoexponential equation, and the lifetimes ranged between 3.9 and 4.4 ns (Table 1). Similarly, all of the anisotropy decays (lower panels) were well fit to a model-free nonassociative biexponential equation (eq 2); thus, like the TRFA analysis of cAPK, the anisotropy decay profiles

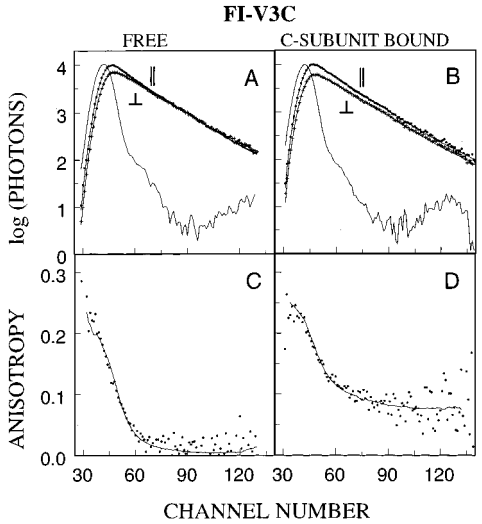

FIGURE 4: Emission and anisotropy decay of free (panels A and C) and C-subunit-bound (panels B and D) Fl-V3C PKIα. The upper panels (A and B) show the polarized excitation lamp flash (thin line) and fluorescence emission monitored both parallel (||) and perpendicular (⊥) to the excitation. The time-resolved anisotropy decay single datum points and the smooth line through these points are plotted in panels C and D. The best-fit parameters for this line were calculated from a double-exponential equation (eq 2) and are listed in Table 1. The procedures used to obtain the results and to fit the data are described in the Experimental Procedures section.

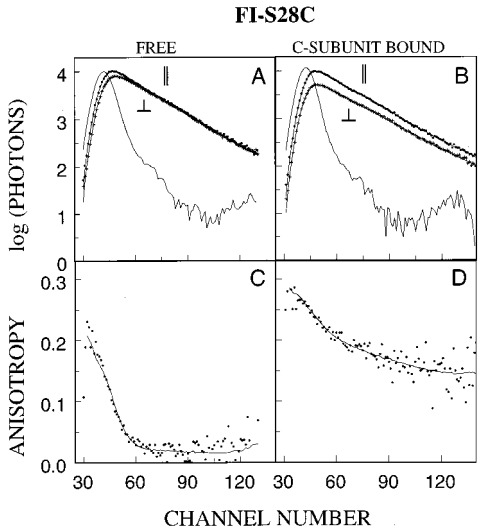

FIGURE 5: Emission and anisotropy decay of free and C-subunit-bound Fl-S28C PKIα. Details of each panel can be found in the legend to Figure 4.

are associated with fast and slow decay processes. The best-fit parameters for the decays are summarized in Table 1.

Free in solution, the anisotropy decay profiles of the labeled-PKIα mutants are very similar to one another. Each is dominated by 0.8−1.4 ns fast anisotropy decay processes (ϕ_F), which accounts for 51−63% of the total decay (Table 1). These ϕ_F's are significantly smaller than the ϕ_F's associated with the sites of cysteine substitution and FM conjugation on the flexible N- and C-terminal domains of the C-subunit (1.8−2.0 ns; ref *13*). On the basis of the FM-labeled cAPK TRFA results (*13*), free PKIα would appear to be associated with substantial backbone flexibility around all three sites examined. Also, suggestive of a high level of flexibility around each site of PKIα mutation and conjugation are the high amplitudes of the fast decay processes (0.18−

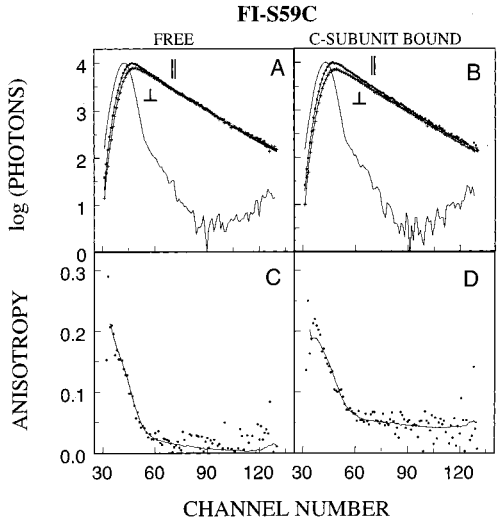

FIGURE 6: Emission and anisotropy decay of free and C-subunit-bound Fl-S59C PKIα. Details of each panel can be found in the legend to Figure 4.

0.22) that are more than twice the r_F values observed for the flexible N- and C-terminal domains of the C-subunit (0.075−0.089) (*13*).

As an aside, the ϕ_F value of FI-V3C (1.4 ns) was significantly higher than that of either FI-S28C (1.0 ns) or FL-S59C (0.8 ns). The higher value of ϕ_F may reflect the more ordered α-helical character of residues 1−13 (Figure 1) that was revealed by NMR spectroscopy (*8*). However, confirmation of the ability of TRFA to report on differential flexibility associated with secondary structural elements obviously requires a more systematic site-directed labeling and TRFA analysis.

In addition to the dominant fast processes, much lower amplitude (4−11%) and slower (13−17 ns) decay processes (ϕ_S) were observed in the free PKIα decay profiles. These slower decay rates are about the same magnitude as the rotational correlation time (11.2 ns) predicted by the Stokes−Einstein equation using the published hydrodynamic radius of PKIα (22.1 Å; ref *6*). Consequently, as previously observed with the TRFA analysis of the FM-labeled C-subunit mutants, these ϕ_S's most likely represent whole-body PKIα rotational diffusion, and the binding of PKIα to the C-subunit of cAPK should be associated with an increase in the ϕ_S values for the three PKIα conjugates. Indeed, the specific ϕ_S values increased from 13−17 ns to 32−40 ns (Table 1), which is about what would be expected (43 ns) for the hydrodynamic radius of the PKIα−C-subunit complex (34.7 Å; ref *20*).

With regard to the fast anisotropy decay parameters, the effects of C-subunit binding to the labeled mutants were complex and depended upon the site of mutation. For FI-S59C, C-subunit binding minimally altered the anisotropy decay parameters. Only ϕ_F, the fast rotational correlation time, was affected, and it increased slightly from 0.8 to 1.1 ns (Table 1). Although this increase is consistent with a small decrease in the backbone flexibility around the site of conjugation, its value is significantly less than the ϕ_F's associated with the sites of fluorescein−maleimide conjugation on the flexible N- and C-terminal domains of the fluorescein−maleimide-labeled C-subunit of cAPK (1.8−2.0) (*13*).

For FI-V3C, binding to the C-subunit was associated with a small increase in ϕ_F (from 1.4 to 1.6 ns) and about a 32% decrease in the amplitude of the fast decay processes, r_F (0.22 to 0.15; Table 1). Although these binding-dependent changes are both in the direction of decreased backbone flexibility, they are still below what was observed for the flexible N- and C-termini of the fluorescein−maleimide-labeled C-subunit (ϕ_F, 1.8−2.0 ns; r_F, 0.075−0.089; ref *13*). V3 and presumably V3C are part of the cAPK-binding domain because PKIα(1−24) has 1.8-fold higher affinity toward the C-subunit than PKIα(5−24). Consequently, one would expect the domain around V3C to interact with the C-subunit, and therefore, there should be a decrease in the conformational flexibility in this region upon binding. With the focus more on the binding-dependent decrease in r_F, the results would thus suggest that C-subunit binding decreases the backbone flexibility of the region around V3C.

The fast and very fast TRFA decay parameters associated with FI-S28C, on the other hand, were highly perturbed by PKIα binding to the C-subunit. The ϕ_F increased from 1.0 to 1.7 ns, r_F, the amplitude of the fast decay processes, decreased ∼68% (from 0.22 to 0.07), and r_{VF}, the amplitude of the very fast anisotropy decay processes, decreased by ∼42% (from 0.12 to 0.07; Table 1). Also, as mentioned above, the fluorescence lifetime (τ) increased from 4.0 to 4.4 ns (Table 1). Together, these results strongly indicate that the binding was associated with an increase in the hydrophobicity of the microenvironment around the probe (producing $\uparrow \tau$) and with a decrease in the local side-chain and tether-arm mobility (producing a $\downarrow r_{VF}$). These effects can be explained if the fluorescein conjugated to S28C became sandwiched between the C-subunit and PKIα or if a portion of PKIα folded back over the fluorescein moiety. In either case, a highly rotationally constrained fluorescein conjugated would most likely be associated with a region of limited backbone flexibility, and thus, the region around S28C probably becomes relatively immobilized upon PKIα binding to the C-subunit of cAPK.

DISCUSSION

Selected single-point mutations of PKIα (V3C, S28C, and S59C) in combination with TRFA were used to monitor the conformational flexibility of PKIα upon binding to the C-subunit of cAPK. The results reveal that PKIα in the free-solution state is highly flexible. However, upon binding to the C-subunit, the N-terminal portion including and flanking the cAPK inhibitory binding domain becomes less flexible and presumably structured while the C-terminus, which includes the helical NES domain, remains largely flexible and presumably unstructured (Figure 7).

The highly flexible character of free PKIα is supported by NMR (*8*), CD (*21*), and FTIR (*21*) studies. In addition, gel filtration data (*6*) indicates the hydrodynamic radius of PKIα to be 22.1 Å, ∼36% greater than what would be predicted by the Stokes−Einstein equation for a compact, spherical peptide with the molecular weight of PKIα (8 kDa). The limited degree of secondary structure and the extended conformation of PKIα again are consistent with PKIα existing in a flexible and unstructured state (Figure 7).

Further support for the differential changes in PKIα's flexibility upon cAPK binding comes from inference and

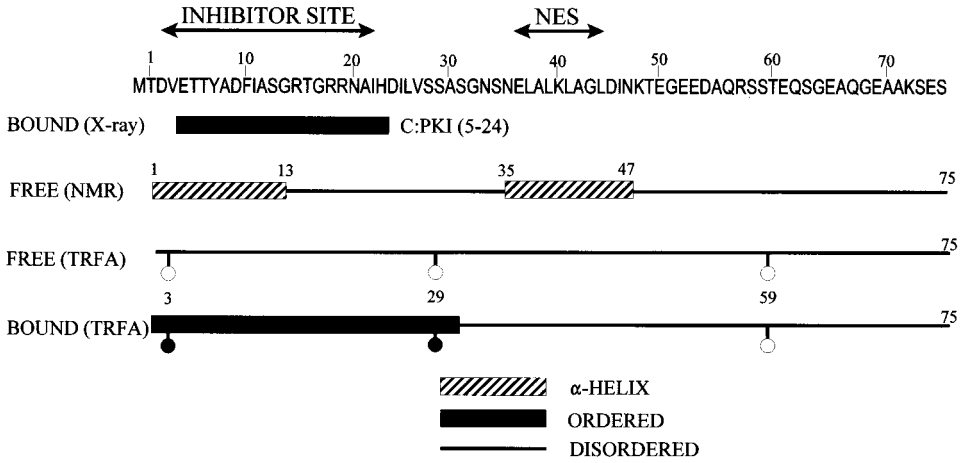

FIGURE 7: Summary of the regional conformational order/disorder of PKIα and PKIα(5−24) in the free-solution and in the bound states as deduced from X-ray crystallography, NMR, and TRFA spectroscopes.

unpublished NMR studies. First, by inference, because the Val^3 and the Ser^{28} sites of mutation are in or flank the PKIα's inhibitor-binding domain, direct peptide−protein interaction should be associated with a loss of conformational flexibility around these sites of mutation and labeling upon C-subunit binding. Second, the flexibility of C-terminus, which includes the NES, is confirmed by unpublished NMR studies by us with ^{15}N-PKIα that reveal that the C-terminus of PKIα, including Ser^{59}, does not interact with the C-subunit and retains its unstructured character (unpublished results).

PKIα is not the only regulatory peptide/protein that is associated with a binding-dependent disorder−order transition. p21, the cylin-dependent kinase (Cdk) inhibitor, which is involved with p53-dependent cell cycle control, lacks stable secondary or tertiary structure in the free-solution state (*2*). Upon binding to one of its biological targets, Cdk, the N-terminal domain of p21, which includes the Cdk inhibitory domain, becomes structured on the basis of NMR spectroscopy. In addition to p21, FlgM, an inhibitor of sigma 28, which is a transcription factor for the expression of bacterial flagella and chemotaxis genes, is also largely unfolded and conformationally dynamic in the free-solution state (*22*). Once again, upon binding to its biological target, sigma 28, its last 57 amino acids, which includes the sigma 28 binding domain, adopt a structured conformation (*22*). It is reasonable to infer that the binding of PKIα only or the PKIα−C-subunit complex to CMR1, a nuclear export protein and the putative target of NES, will represent another example of a disorder−order transition associated with target site binding.

Two technical comments need to be made. First, no "shape comformers", as suggested by an earlier study of PKIα (*23*), were detected in the work described above. This was mainly because only PKIα that migrated through a gel filtration column with an apparent molecular weight of 22 000 was utilized. This form of PKIα should correspond to the previously designated "I" conformer (*23*). Second, comparison with our previous efforts to examine the regional flexibility of the C-subunit using FM-labeled-substituted cysteines suggests differences in the sensitivity of the r_F and the ϕ_F terms to monitor backbone flexibility in the two studies. The r_F terms from the FI-labeled-PKIα mutants discussed above appear to be more sensitive to the backbone flexibility than the ϕ_F terms, while the opposite was observed with the FM-labeled C-subunit mutants (*13*). It is unclear whether these differences are due to the dissimilar linkage arms (acetamidothioether versus the rotationally constrained succinimidylthioether), the differences in size of the peptide/protein examined (8 versus 40 kDa), or the level of secondary and tertiary structure (low versus high). Further work is clearly required to resolve this issue.

In summary, we examined with a combination of site-directed labeling and TRFA the backbone flexibility around three residues of PKIα (Val^3, Ser^{28}, and Ser^{59}) that were in either the free or the cAPK-bound states. The results confirm that the cAPK-binding domain of PKIα extends from its N-terminus to residues beyond Ser^{28} but stops well before Ser^{59}, which is part of a highly flexible region even when it is bound to the C-subunit. Thus, even bound to the C-subunit, the C-terminal region of PKIα, which includes a NES, retains its flexibility, presumably for optimal binding to CRM1, its biological target.

ACKNOWLEDGMENT

We would like to thank Siv Garrod for performing the mass spectroscopy on the PKIα proteins and Teresa Clifford and Cindy Gribskov for the preparation of the recombinant C-subunit.

REFERENCES

1. Vajda, S., Weng, Z., Rosenfeld, R., and DeLisi, C. (1994) *Biochemistry 33*, 13977−13988.
2. Kriwacki, R. W., Hengst, L., Tennant, L., Reed, S. I., and Wright, P. E. (1996) *Proc. Natl. Acad. Sci. U.S.A. 93*, 11504−11509.
3. Jorgensen, C. I., Kallipolitis, B. H., and Valentin-Hanser, P. (1998) *Mol. Microbiol. 27*, 41−50.
4. Fantozzi, D. A., Harootunian, A. T., Wen, W., Taylor, S. S., Feramisco, J. R., Tsien, R. Y., and Meinkoth, J. L. (1994) *J. Biol. Chem. 269*, 2676−2686.
5. Walsh, D. A., Ashby, C. D., Gonzalez, C., Calkins, D., Fischer, E. H., and Krebs, E. G. (1971) *J. Biol. Chem. 246*, 1977−1985.
6. Walsh, D. A., Angelos, K. L., Van Patten, S. M., Glass, D. B., and Garetto, L. P. (1990) in *Peptides and Protein Phosphorylation* (Kemp, B. E., Ed.) pp 43−84, CRC Press, Inc., Boca Raton, FL.
7. Wen, W., Meinkoth, J. L., Tsien, R. Y., and Taylor, S. S. (1995) *Cell 82*, 463−473.
8. Hauer, J. A., Barthe, P., Taylor, S. S., Parello, J., and Padilla, A. (1999) *Protein Sci*. (in press).

9. Knighton, D. R., Zheng, J., Ten Eyck, L. F., Xuong, N.-h., Taylor, S. S., and Sowadski, J. M. (1991) *Science 253*, 414−420.
10. DeLecea, L., Criado, J. R., Rivera, S., Wen, W., Soriano, E., Henriksen, S. J., Taylor, S. S., Gall, C. M., and Sutcliffe, J. G. (1998) *J. Neurosci. Res. 53*, 269−278.
11. Marchetto, G., and Henry, H. (1997) *Endocrine 6*, 5−10.
12. Wen, W., Taylor, S. S., and Meinkoth, J. L. (1995) *J. Biol. Chem. 270*, 2041−2046.
13. Gangal, M., Cox, S., Lew, J., Clifford, T., Garrod, S. M., Aschbaher, M., Taylor, S. S., and Johnson, D. A. (1998) *Biochemistry 37*, 13728−13735.
14. Kunkel, T. A., Benebek, K., and McClary, J. (1991) in *Methods in Enzymology* (Miller, J. H., Ed.) pp 125−139, Academic Press, Inc., San Diego, CA.
15. Wen, W., and Taylor, S. S. (1994) *J. Biol. Chem. 269*, 8423−8430.
16. Yonemoto, W., Garrod, S. M., Bell, S. M., and Taylor, S. S. (1993) *J. Biol. Chem. 268*, 18626−18632
17. Cook, P. F., Neville, M. E., Vrana, K. E., Hartl, F. T., and Roskoski, R. (1982) *Biochemistry 21*, 5794−5799.
18. Yguerabide, J. (1972) *Methods Enzymol. 26*, 498−578.
19. Beechem, J. M., Gratton, E., Ameloot, M., Knutson, J. R., and Brand, L. (1991) in *Topics in Fluorescence Spectroscopy* (Lakowicz, J. R., Ed.) pp 241−305, Plenum Press, New York.
20. Herberg, F. W., and Taylor, S. S. (1993) *Biochemistry 32*, 14015−14022.
21. Thomas, J., Van Patton, S. M., Howard, P., Day, K. H., Mitchell, R. D., Sosnick, T., Trewhella, J., Walsh, D. A., and Maurer, R. A. (1991) *J. Biol. Chem. 266*, 10906−10911.
22. Daughdrill, G. W., Chadsey, M. S., Karlinsey, J. E., Hughes, K. T., and Dahlquist, F. W. (1997) *Nat. Struct. Biol. 4*, 285−291.
23. McPherson, J. M., Whitehouse, S., and Walsh, D. A. (1979) *Biochemistry 18*, 4835−4845.

BI983074K